IV International Conference on Computational Methods for Coupled Problems in Science and Engineering
COUPLED PROBLEMS 2011
M. Papadrakakis, E. Oñate and B. Schrefler (Eds)

MODELING OF AIRBLAST PROPAGATION THROUGH AN ENCLOSED STRUCTURE

JESSE A. SHERBURN*,†, DONALD H. NELSON†, CAREY D. PRICE†
AND THOMAS R. SLAWSON†

† U.S. Army Corps of Engineers
Engineer Research and Development Center
3909 Halls Ferry Rd., Vicksburg, MS 39180, USA
e-mail: {jesse.a.sherburn, donald.h.nelson, carey.d.price, thomas.r.slawson}@usace.army.mil

Key words: Fluid-Structure Interaction, CTH, DYSMAS, Confined Airblast

Abstract. *The ability to model explosively formed shock waves propagating through a structure is of particular interest to engineers concerned with structural responses to blasts. Accurate peak pressure and impulse values are critical to understanding blast loads on structures and predicting the resulting structural behavior, but are sometimes difficult to determine analytically. Experiments are necessary to determine the true structural response, but the experiments alone may not identify all the details involved in an explosive event that may be important for design purposes. When tied to experiments, computational modeling of explosive events can be an invaluable tool for an engineer. The most difficult part of modeling structural response to a close-in explosive event is capturing the fluid-structure interaction of the resulting flow of the detonation products. In this paper, we compare the results of numerical simulations of an explosive experimental event in an enclosed structure, or "attic space", using two different computational codes, CTH and DYSMAS. Both adequately model the explosive event in attic space when compared to the experiment. We also compare the two codes' ability to produce explosive-induced pressure-time histories in the free field. The advantage of using a coupled code like DYSMAS is that structural response can be more accurately captured than by using a hydrocode like CTH alone. The differences between the two codes' ability to model the event are analyzed and described as well as a general description of the shock wave propagation in the attic space.*

1 INTRODUCTION

Designing enclosed structures to withstand explosively-generated shock waves presents many difficulties for the military structural engineer. The original studies on confined blast started in World War II, but the first useful study published was that of Weibull [1] in 1968 that correlated peak quasi-static pressure versus the charge weight for a series of TNT charges detonated within a vented enclosure. Since then numerous studies were conducted to understand confined blast on structures [2-6]. Some recent studies [7-8] have numerically modeled confined explosive events for understanding the structural loading and mitigation techniques.

An engineer needs to know the blast pressure-time history, or as a minimum the pressures and impulses a structure will need to withstand, in order to produce an adequate design. Analytical methods work for simple structures; but in complicated structural configurations, it can be difficult or impossible to predict localized loading throughout the structure. With experimental validation, computational models have the ability to aid the engineer in understanding explosively-generated loads on a complicated structure. Many different tools exist such as LS-DYNA, AUTODYN, ABAQUS, and others, but for this study CTH and DYSMAS were used to perform simulations on a structure undergoing close-in airblast. CTH, an advanced Eulerian hydrocode developed by Sandia National Laboratories for the purpose of modeling materials under large deformations, was used for analysis of shock propagation through the structure [9]. In contrast to CTH, DYSMAS is a coupled Eulerian-Lagrangian code that allows the fluid and the structure to be modeled separately. DYSMAS was originally developed by the United States Navy for modeling under water explosions on structures [10-11]. This study performed simulations on an enclosed structure using CTH and DYSMAS and compared the results to experimental data. Simple free field calculations in open air were performed to compare CTH's and DYSMAS's ability to propagate airblast. This paper shows the merits of using a coupled fluid-structure code like DYSMAS for this type of scenario.

2 MODEL SETUP

2.1 Experimental setup

Figure 1 shows the experimental scale model of the structure investigated in this study. The structure consisted of a roof deck suspended 0.188 m above a ceiling deck, forming an attic space between. The structural members (frames and purlins) were simple rectangular cross sections. A mild steel was used in order to produce a near non-responding reaction structure in which to measure the pressure wave as it propagated and reflected through the attic space. The final dimensions of the structure measured 2.3 m in width, 0.91 m high at the ridgeline, and 2.5 m in length. A 0.17 m circular hole was cut (shown in Figure 1) in the upper roof to simulate the breeched area in the roof and to remove the complexity of having to model the effects of breaching on the blast propagation into the attic space, and a spherical RDX-based explosive was placed just above the center of the hole and flush with the roof line. The amount of explosive used in this study was 36.45 g.

Figure 1: Elevation and plan view of experimental structure.

The pressure-time histories were measured by pressure gages on the top of the ceiling deck as shown in Figure 2. The only pressure gage that will be discussed in this study is gage 12 which is located on top of the ceiling deck in the center of the structure, as shown in Figure 2. Figure 2 also shows the charge location relative to gage 12.

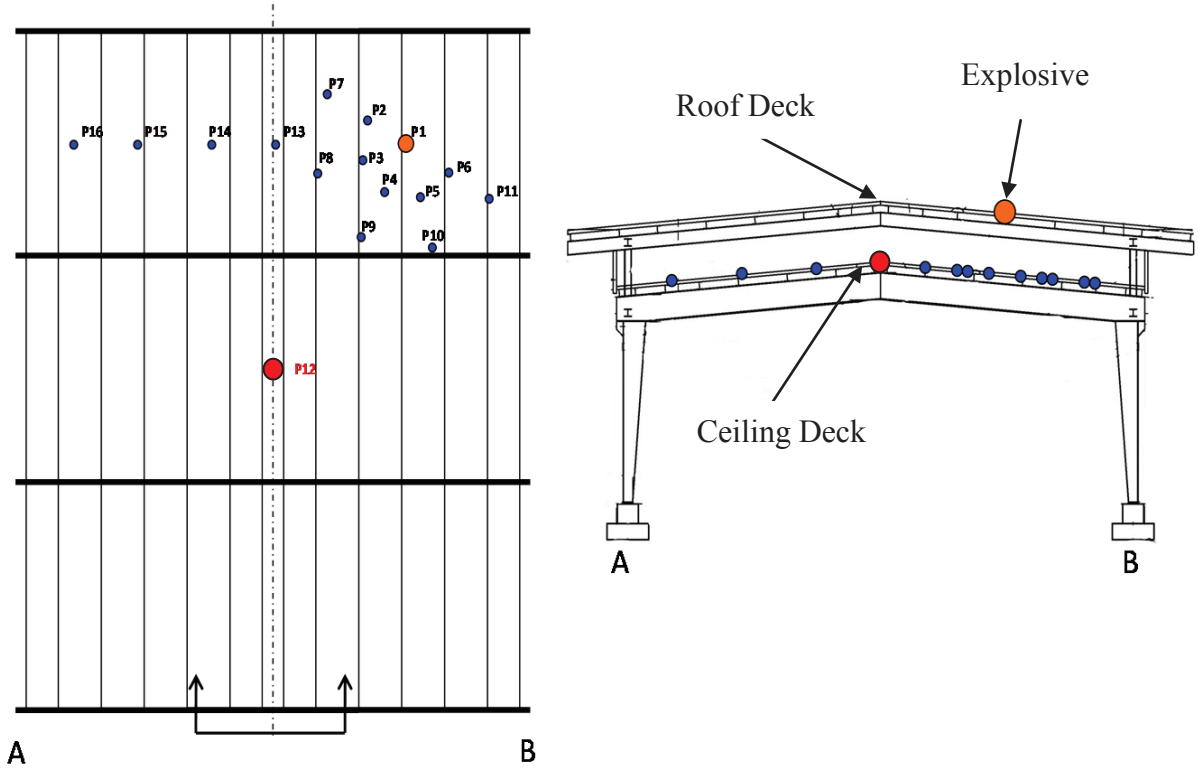

Figure 2: Plan and elevation views of gage layout. The large orange circle represents explosive location. The gage under consideration is in the center of the structure on top of the ceiling deck (large red dot). Note the simulation setup is mirror image of this gage layout.

2.2 CTH model

The CTH model incorporated a simplified upper portion of the experimental structure discussed in section 2.1. Figure 3 displays a three-dimensional view of the CTH model setup with the hole and the spherical charge clearly shown. The Jones-Wilkins-Lee (JWL) equation-of-state (EOS) was used to model the charge, and the structure's material used a SESAME tabulated EOS with a simple elastic-plastic von mises yield model for mild steel. The JWL EOS parameters are listed in Table 1. Air was also included using the SESAME tabulated EOS in CTH in order to properly propagate the pressure wave through the structure. The total size of the CTH model was identical to that of the experimental structure discussed in section 2.1. The domain size was limited to 750 x 750 x 200 cells, or 3.75 m x 3.75 m x 1.0 m. The sides and top boundary conditions were transmitting boundaries while the bottom boundary was a wall condition. A mesh sensitivity study was conducted to determine an adequate mesh size for accuracy and computational efficiency. The study determined that a uniform mesh with a cell size of 0.005 m for a total of 112.5 million cells over the domain fulfilled the balance between accuracy and efficiency. Stationary tracer particles were placed in the same

gage locations as those in the experimental model shown in Figure 2. The simulation was conducted in two phases. First, a one-dimensional simulation propagated the initial pressure wave up until the time just before it would impinge on the structure. Secondly, the one-dimensional results were rezoned and placed into the three-dimensional domain and the simulated propagation was allowed to continue. Stationary tracer particles at corresponding gage locations recorded the pressure-time histories throughout the simulation.

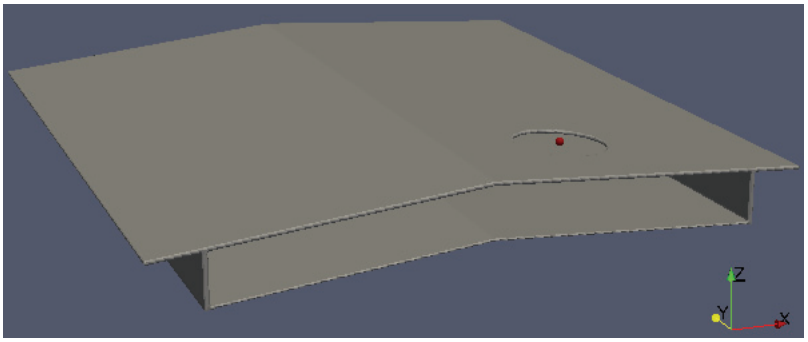

Figure 3: Simplified simulation of the attic space structure. Note the location of the charge above the hole.

Table 1: JWL parameters used for modeling the explosive.

Constant	Value
Density (g/cm^3)	1.601
AG (MPa)	6.0977×10^5
BG (MPa)	1.295×10^4
Omega	0.25
R1	4.5
R2	1.4

2.3 DYSMAS model

The DYSMAS model included the same simplified attic space as the CTH model. The main difference between the CTH model and the DYSMAS model was the DYSMAS model had the solid and fluid parts separated. The fluid part, or Eulerian domain, was where the air and the explosive detonation products were modeled. The size of the Eulerian domain was identical in size to the CTH model described in section 2.2. The domain boundaries were identical to the CTH simulation. Air was modeled using a gamma law EOS, and the explosive was modeled with the JWL parameters in Table 1. The solid part, or Lagrangian structure, was modeled using a near uniform finite element mesh. Figure 4 displays the mesh which consisted of about 30,000 shell elements with each element having an average side length of 0.02 m and a shell thickness of 0.0127 m. The same material model for mild steel was used for the structure. The Lagrangian structure was then placed in the Eulerian domain in the same configuration as the CTH model. DYSMAS requires the elements that were in contact with the fluid domain must be specified as a wetted element. This specification of wetted elements allows DYSMAS to handle the coupled fluid-structure interaction when a pressure wave and/or detonation products impinges on a structure. Just like the CTH calculation a one-dimensional Eulerian simulation was performed for the initial expansion of the pressure wave and detonation products and then was rezoned into the three-dimensional Eulerian domain.

The simulation was then allowed to continue to completion. Stationary tracer particles at analogous CTH locations were placed in the Eulerian DYSMAS domain. An added benefit to DYSMAS was an element's history near a pressure gage location could also be recorded to measure exactly what pressure loads the structure endured.

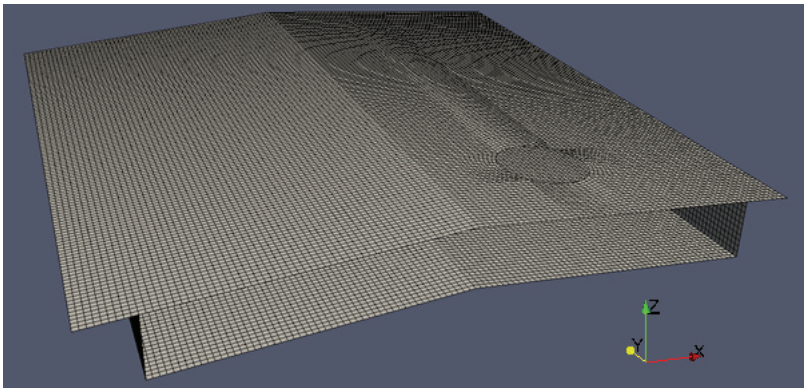

Figure 4: Lagrangian mesh used for the DYSMAS calculation.

2.4 Free field model

Simple free field simulations were conducted in both CTH and DYSMAS in order to compare the propagation of a pressure wave through air. This was to ensure they could be compared directly. The two-dimensional axisymmetric domain consisted of a 1.0 m x 2.0 m size with the explosive at the center. The same explosive weight was used (36.45 g) in the free field simulations as the previously described CTH and DYSMAS calculations. The uniform cell size was identical to the CTH and DYSMAS calculations (0.005 m) and used the same rezoning technique. The rezoning in the free field case was done from a one-dimensional domain to a two-dimensional domain. A single stationary tracer particle was placed 0.5 m away from the explosive's center and recorded the pressure-time history.

3 RESULTS

3.1 Free field results

The free field simulations compared adequately between CTH and DYSMAS for this scenario. Figure 5 shows the pressure-time history at the tracer particle for both CTH and DYSMAS. The arrival times were comparable with CTH arriving slightly earlier and the CTH peak pressure was also slightly smaller in magnitude. These differences were expected because CTH and DYSMAS used a different EOS for air. The SESAME tabulated EOS used by CTH is more realistic (i.e., more physics included) than the gamma law, but for the purposes of this study the similarity between the results was satisfactory.

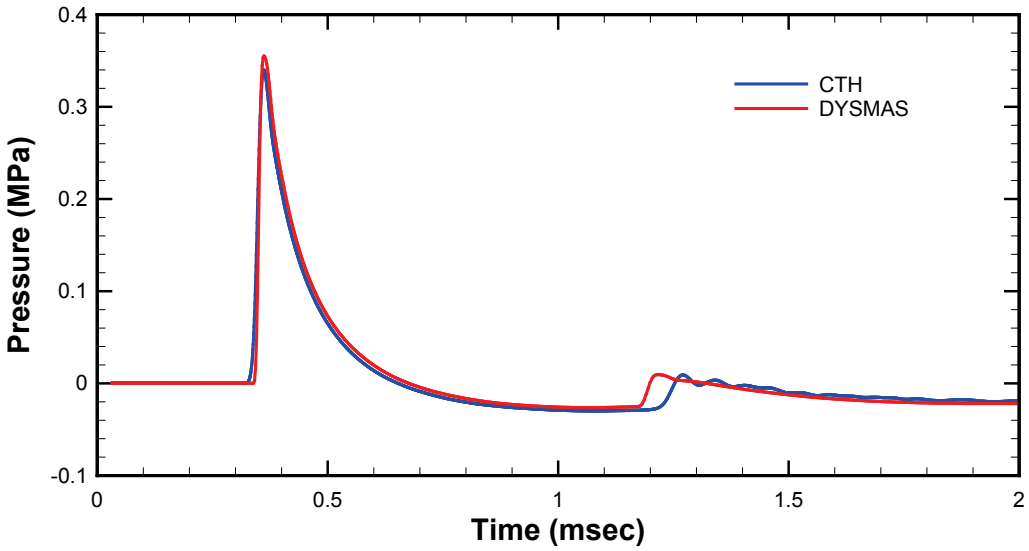

Figure 5: Free field pressure-time histories for CTH and DYSMAS located 0.5 m away from charge center.

Figure 6 shows the pressure field contours for the CTH and DYSMAS free field simulations at time 1.0 msec. The pressure contours were near identical in size and shape. CTH included more fluctuations in pressure due to the presence of more Richtmyer-Meshkov instabilities between the detonation products and the air. The DYSMAS simulation did have some of the instabilities, but not as many as CTH. The second pressure wave was produced by the creation of a low pressure void in the expanding detonation products that eventually collapsed the detonation products inward. The collapse then rebounds to produce the small pressure peak shown in Figure 5 around 1.2 msec. When the second pressure wave passes through the instabilities, the resultant pressure field has a non uniform look as shown in Figure 6a. The DYSMAS detonation products did not have as many instabilities, so the second pressure wave had a near circular shape. The differences between the two simulations were minimal which gave confidence that comparing the loading on the structure would be valid.

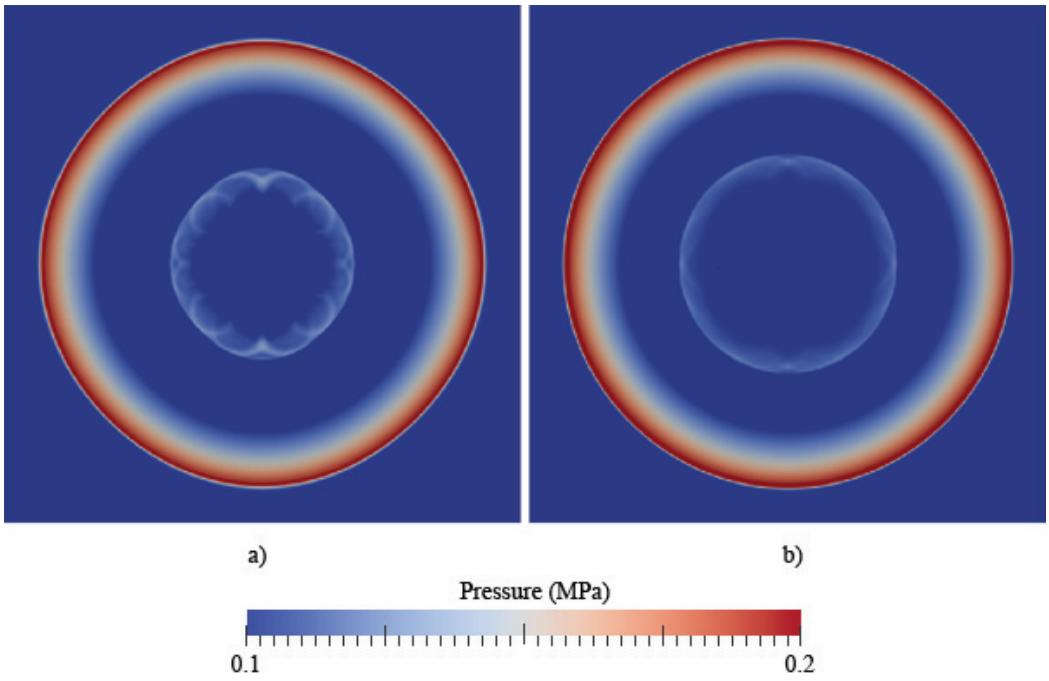

Figure 6: Free field pressure contours at time 1.0 msec for a) CTH and b) DYSMAS.

3.2 CTH and DYSMAS results

The overall response of the simplified CTH and DYSMAS simulations was adequate when compared to the experimental data. There were some differences noted in the initial peak pressures and subsequently the impulse on the structure. Figure 7 shows the detonation products at time equals 2.0 msec. The simulations have similar shapes but have some distinct differences. The overall expanse in the detonation products were the same size but interacted differently on the structure's surface. The detonation products in the CTH calculation tended to adhere to the structure's surface more than the DYSMAS calculation. The DYSMAS detonation products slid fairly well compared to CTH along the roof's surface, as shown in Figure 7b. Inside of the attic space the same adhering happened in CTH, and the detonation products did not get pushed by the sidewall reflected pressure wave as much as the DYSMAS calculation.

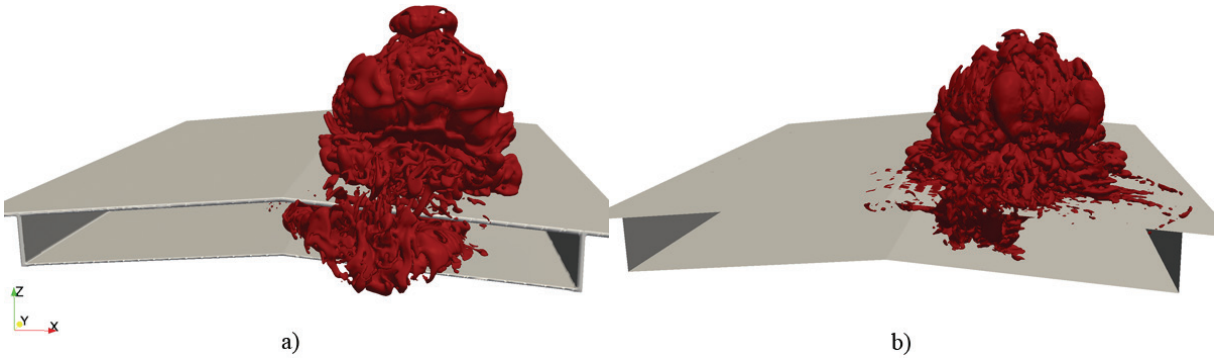

Figure 7: Detonation products at time 2.0 msec for a) CTH and b) DYSMAS.

The pressure field contours at time equals 1.15 msec for the CTH and DYSMAS calculations are shown in Figure 8 for a cross section in the center of the structure. The pressure wave on the top of the roof surface looked identical in both CTH and DYSMAS cases. Inside the attic space the pressure waves had similar magnitudes, but the arrival times of the inner reflected wave were quite different. Some of this was due to the fact that DYSMAS uses a shell element with an assumed thickness for response purposes which made the attic space cross section area slightly larger than the CTH case as shown in Figure 8. This would make the wave reflect quicker in the CTH case.

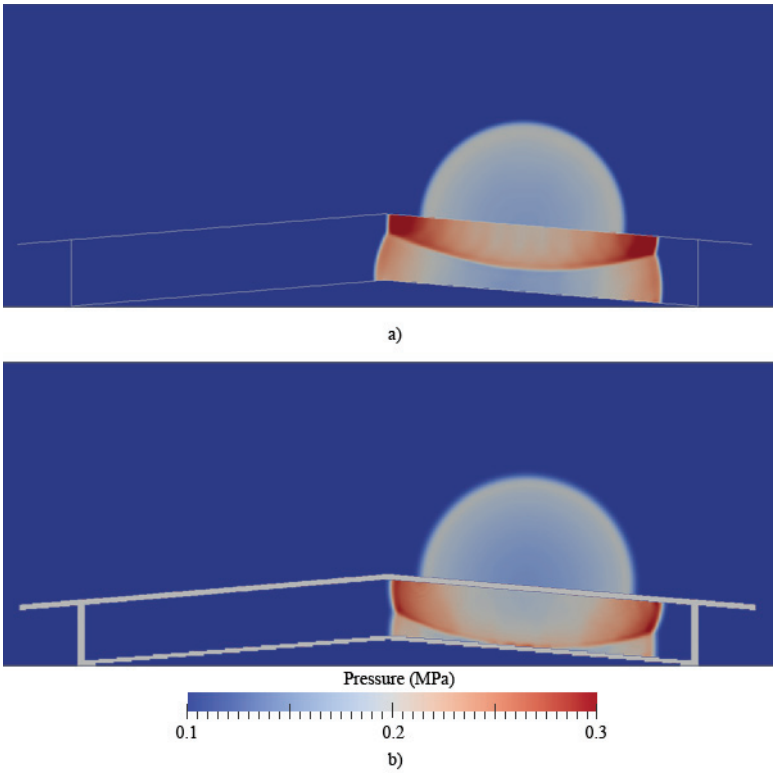

Figure 8: Pressure contours at time 1.15 msec for a) DYSMAS and b) CTH.

Figure 9 displays the pressure-time histories for CTH, DYSMAS, and the experiment at gage 12. Both of the CTH and DYSMAS simulations adequately predicted the character of the pressure-time history of the experiment data. Both the CTH and DYSMAS calculations look smoother because there were no interior frame or purlin members to cause the complex reflections observed in the experimental data, as shown in Figure 9. CTH nearly matched the experimental initial peak pressure at 6.7% higher than the experimental data, while DYSMAS undershot the peak pressure data by 20%. A large difference between the experimental data and the models is the presence of a high secondary peak which shows up in the experimental data at time 2.3 msec and between 2.5 msec and 3.0 msec in CTH and DYSMAS, as shown in Figure 9. The difference between the models and the experiment is clearly shown when impulse-time history is plotted as shown in Figure 10. This secondary peak causes the overall impulse to be much higher in the experimental data, which is the reason the simulations deviate from the experimental impulse shown in Figure 10. The explanation for this

difference could be threefold. First the simplified model in this study may not capture a large reflection off of an interior member that is present in the experimental data. A second explanation is that afterburning effects were not included in the hydrodynamic simulations which would account for the extra pressure in the secondary pressure wave shown in Figure 9. Research has shown afterburning effects in RDX-based explosives can be quite substantial in any enclosed or semi enclosed environment [8]. A third explanation is the JWL EOS did not adequately capture shock propagation through preshocked air which implies the second pressure wave in the simulations did not propagate as quickly as the experimental test. More research needs to be done in order to quantify this difference for this particular structure.

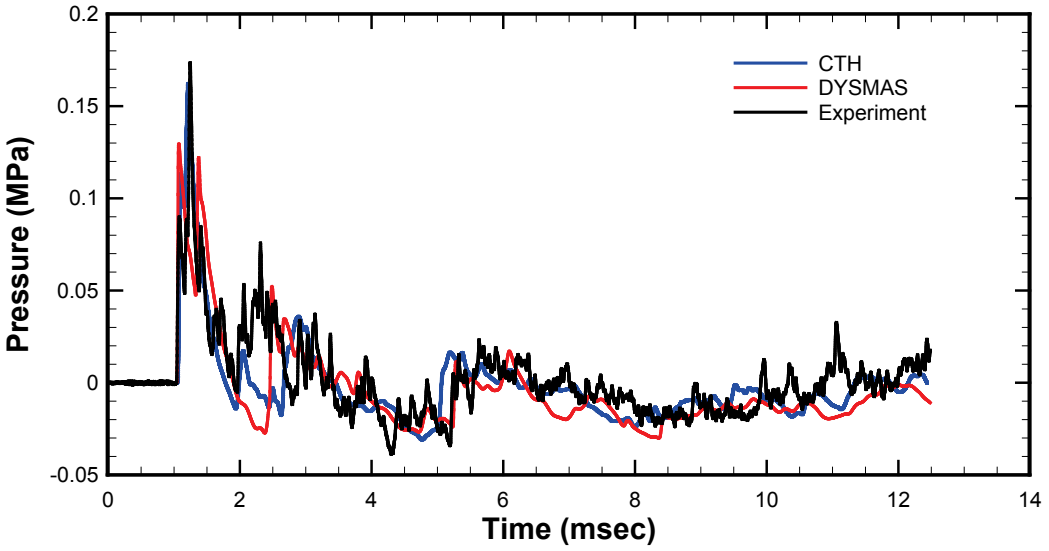

Figure 9: Comparison of pressure-time histories at gage 12 for CTH, DYSMAS, and experiment.

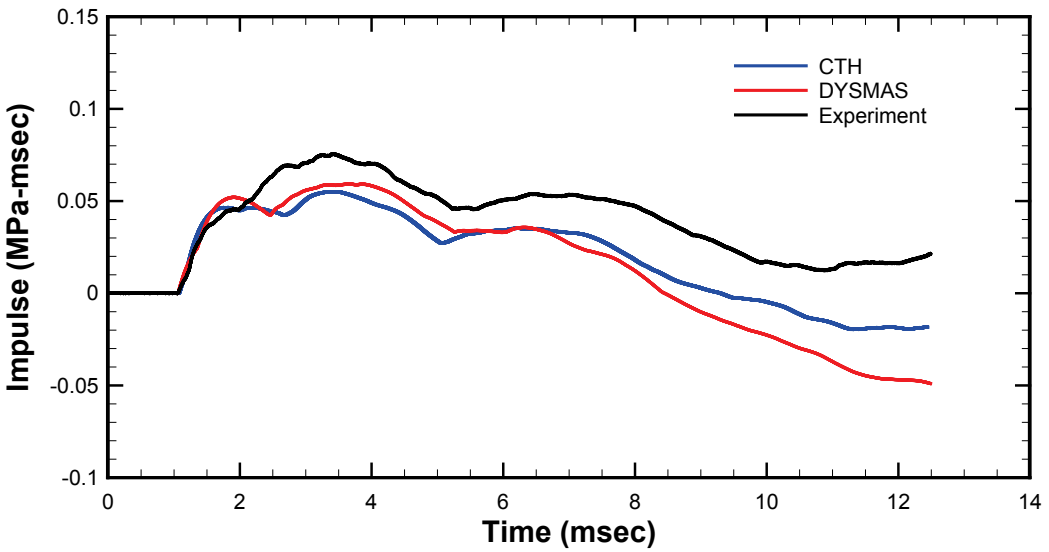

Figure 10: Comparison of impulse-time histories at gage 12 for CTH, DYSMAS, and experiment.

One of the advantages of using a coupled code like DYSMAS is the ability to extract relevant data on the structure being loaded from the finite element mesh. Extracting this data from CTH is impossible due to the fact that the mesh is fixed in space. Figure 11 compares the experimental data, the data extracted from the Eulerian domain tracer, and the data from the element closest to the gage location. The structure's element has about a 12% lower peak pressure than the Eulerian domain tracer which indicates the structure actually feels less of the pressure wave than the Eulerian domain tracer reports. The two data points track similar trends until late time when the structure's element tracts the increasing pressure trend past 8 msec better than the Eulerian domain tracer. Figure 12 displays the matching trend by the impulse-time history. The experimental impulse in earlier times, 2-4 msec, is much higher due to the presence of the larger secondary pressure wave, but the structure's data tracts the experimental impulse trend far better than the Eulerian domain tracer. The Eulerian domain tracer data never turns upward in late times (past 8 msec) like the structure's element and the experimental data. This highlights the fact that the structure responds differently than a tracer in the Eulerian domain reports, which shows the importance of modeling the fluid and the structure separately.

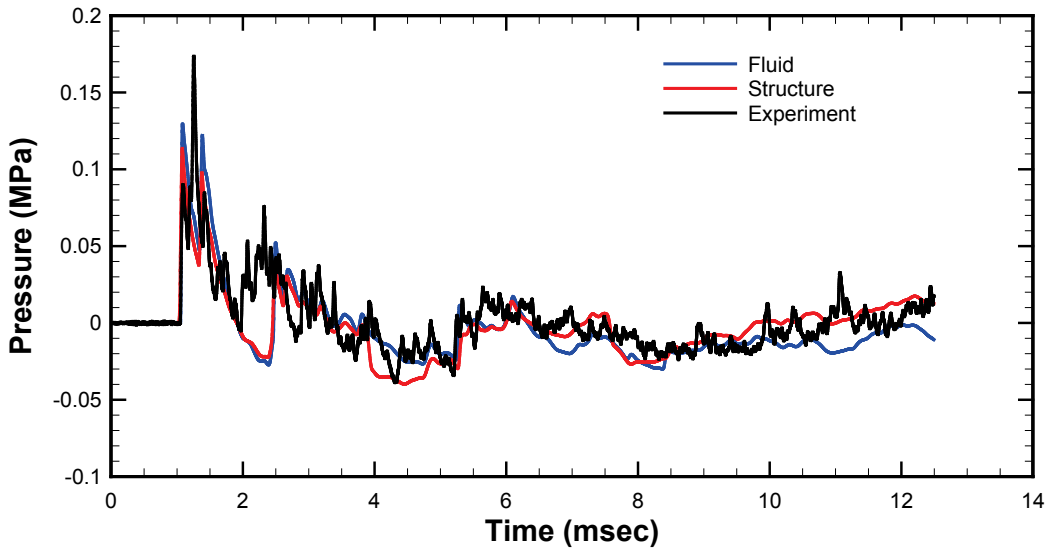

Figure 11: Comparison between fluid and structure pressure-time histories at gage 12 for the DYSMAS calculation.

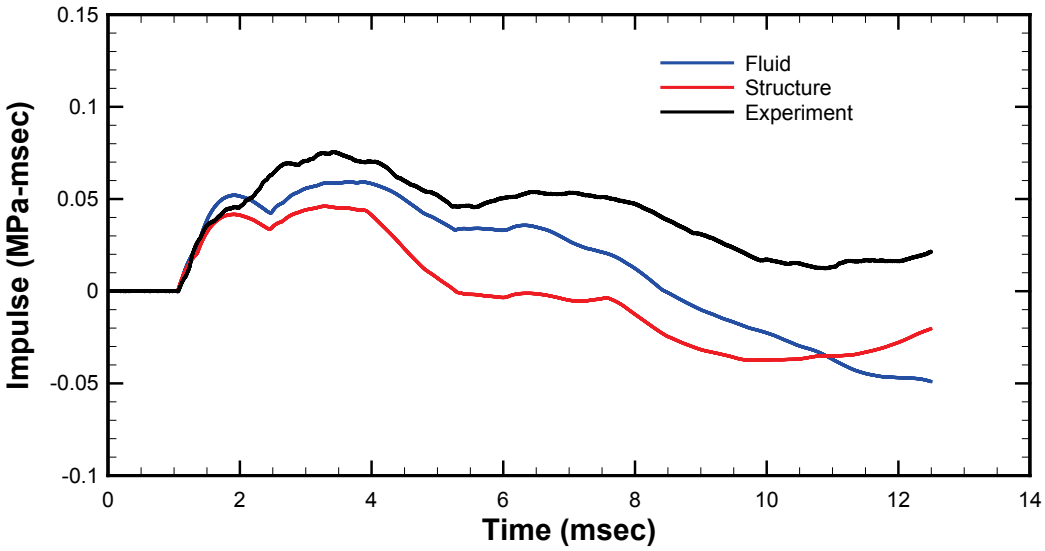

Figure 12: Comparison between fluid and structure impulse-time histories at gage 12 for the DYSMAS calculation.

4 CONCLUSIONS

For the scenario presented in this paper, CTH and DYSMAS both propagated the pressure wave through the attic space adequately compared to the experimental data. DYSMAS had the advantage of more accurately modeling the structure's response to the explosively-generated pressure wave. The comparison of the experimental pressure-time history and impulse-time history results to the simulations allows the design engineer to confidently design a real responding structure with the simulation data. Now that the simulations had success matching the experimental data, different loadings could be tested in DYSMAS on the structure that may be helpful for the design engineer.

This was an initial effort in modeling the attic space that can be extended in complexity in a few different ways. First, the internal members need to be modeled in order to capture the complex reflections present in the attic space. Second, the effect of afterburning needs to be investigated and modeled in order to quantify its effects on the pressure wave and impulse. A third area of future study is the possible EOS issues in the preshocked attic space. A final area of study is to use DYSMAS to study the roof breaching effects on the attic space in a full scale event.

5 ACKNOWLEDGEMENTS

Permission to publish was granted by the Director, Geotechnical & Structures Laboratory. All simulations were performed on Department of Defense Supercomputer Resource Center high performance computers.

REFERENCES

[1] Weibull, H.R.W. Pressures recorded in partially closed chambers at explosion of TNT charges. *Ann. N. Y. Acad. Sci*. (1968) **152**:256-261.

[2] Baker W.E., Anderson Jr., C.E., Morris, B.L and Wauters D.K. Quasi-static pressure, duration and impulse for explosions (e.g. HE) in structures. *Int. J. Mech. Sci.* (1983) **25**:455-464.

[3] Kingery, C.N., Schumacher, R. and Ewing Jr., W.O. Internal pressure from explosions in suppressive structures. Memorandum Report ARBLRL-MR-02848, U.S. Army Ballistic Research Laboratory, Aberdeen Proving Ground, MD (1978).

[4] Esparza, E.D., Baker, W.E. and Oldham G.A., Blast pressures inside and outside suppressive structures. Report EM-CR-76042, Edgewood Arsenal, Aberdeen Proving Ground, MD (1975).

[5] TM5-1300, Structures to resist the effects of accidental explosions. U.S. Departments of the Army, Navy and Air Force (1969).

[6] Beshara, F.B.A. Modelling of blast loading on aboveground structures-II. Internal blast and ground shock. *Comp. Struct.* (1994) **51**(5):597-606.

[7] Gelfand, B.E., Silnikov, M.V. and Chernyshov, M.V. On the efficiency of semi-closed blast inhibitors. *Shock Waves* (2010) **20**:317-321.

[8] Togashi, F., Baum, J.D., Mestreau, E., Löhner, R. and Sunshine, D. Numerical simulation of long-duration blast wave evolution in confined facilities. *Shock Waves* (2010) **20**:409-424.

[9] McGlaun, J.M., Thompson, S.L. and Elrick, M.G. CTH: A three-dimensional shock wave physics code. *Int. J. Impact Eng.* (1990) **10(**1-4):351–360.

[10] Naval Surface Warfare Center (NSWC) Indian Head. *Gemini User's Manual, Release 5.00.00*. 10 May 2010.

[11] Naval Surface Warfare Center (NSWC) Indian Head. *DYNA3D: A Nonlinear, Explicit, Three-Dimensional Finite Element Code for Solid and Structural Mechanics, User's Manual*. July 2009.